Improving 3D MR Velocity-Vector Field Mapping by Divergence-Free Image Reconstruction

J. Busch[1,2], D. Giese[1,3], L. Wissmann[1], and S. Kozerke[1,3]

[1]Institute for Biomedical Engineering, University and ETH Zurich, Zurich, Switzerland, [2]Ruprecht-Karls University Heidelberg, Heidelberg, Germany, [3]Division of Imaging Sciences and Biomedical Engineering, King's College London, London, United Kingdom

Introduction

Phase-contrast magnetic resonance imaging (PC-MRI) provides time-resolved 3D information of velocity fields of flowing blood in vessels. It has however been noted that system imperfections including eddy current related phase offsets, sample noise, displacement and partial volume effects can compromise the accuracy of velocity data derived from phase-contrast measurements [1]. If only noise as a source of inaccuracy is considered, statistical methods of streamline generation may be used to improve overall confidence in the vector field visualization [2]. Eddy-current related phase offsets may be measured and corrected for to a certain extent [3], but residual phase errors remain. In contrast to single-slice phase-contrast measurements, three-directional 3D phase-contrast mapping permits incorporation of the physical constraint of approximate incompressibility of blood flow.

The present work introduces divergence-free image reconstruction for 3D phase-contrast vector field mapping based on a synergistic combination of normalized convolution and divergence-free radial basis functions. Using computer simulations and in-vivo data it is demonstrated that vector field divergence arising from measurement imperfections can be significantly reduced resulting in improved vector field representations.

Theory

Velocity vector fields of incompressible fluid flow can be locally approximated by divergence-free radial basis functions [4, 5] according to:

$$\Phi(\vec{r}) = \left[\left(1-\frac{\vec{r}^{\,2}}{2\alpha^2}\right) I + \frac{1}{2\alpha^2}\vec{r}\cdot\vec{r}^{\,T} \right] e^{-\frac{\vec{r}^{\,2}}{2\alpha^2}},$$

where Φ denotes a radial basis function centred at the origin, $\vec{r}$ refers to the position vector, I represents the 3x3 identity matrix and α is a free parameter determining the size of the support of the radial basis function.

In order to account for partial volume effects and background phase noise the method of normalized convolution assigns degrees of certainty to every voxel and limits the neighbourhood of a voxel under consideration for reconstruction [6]. Thereby, the background is eliminated and voxels inside the vessel lumen may be weighted according to their certainty. Furthermore, the applicability of radial basis functions in the vicinity of a point is controlled. Reconstruction of the full vessel lumen is achieved by voxel-wise steps over the full Cartesian-grid the data are sampled on. To eliminate vector-field divergence the three velocity components v_x, v_y, v_z are processed simultaneously using divergence-free matrix-valued basis functions according to:

$$\begin{pmatrix} \Phi(\vec{r}_1-\vec{r}_1) & \Phi(\vec{r}_1-\vec{r}_2) & \dots & \Phi(\vec{r}_1-\vec{r}_N) \\ \Phi(\vec{r}_2-\vec{r}_1) & \Phi(\vec{r}_2-\vec{r}_2) & & \vdots \\ \vdots & \vdots & \ddots & \vdots \\ \Phi(\vec{r}_N-\vec{r}_1) & \dots & \dots & \Phi(\vec{r}_N-\vec{r}_N) \end{pmatrix} \cdot \begin{pmatrix} c_{11} \\ c_{12} \\ c_{13} \\ c_{21} \\ \vdots \\ c_{NN} \end{pmatrix} = \begin{pmatrix} v_x(\vec{r}_1) \\ v_y(\vec{r}_1) \\ v_z(\vec{r}_1) \\ v_x(\vec{r}_2) \\ \vdots \\ v_z(\vec{r}_N) \end{pmatrix}$$

where $v_x(\vec{r}_i)$, $v_y(\vec{r}_i)$, $v_z(\vec{r}_i)$ with $i=1,2,\dots,N$ denote the values of the three velocity components at positions $\vec{r}_i$, whereat $\vec{r}_i$ is a position vector on the grid the data is represented on. Φ refers to the radial basis functions centred at different positions on the grid and c_{11}, c_{12}, ... , c_{NN} are the 3N coefficients which affect the development of the velocity data points into the basis functions Φ.

The definition of the certainty mask is based on the complex difference image averaged over all velocity encoding segments. The radius of the applicability function is chosen as small as possible to reduce reconstruction time but large enough to ensure continuity between neighbouring reconstruction volumes.

Methods

For simulation purposes a data set of a U-bend was generated using Computational Fluid Dynamics (CFD). Gaussian noise was added to obtain realistic signal-to-noise ratios. In-vivo data of the aorta were acquired using a cine 3D phase-contrast sequence in healthy volunteers on a 3T Philips Achieva system (Philips Healthcare, Best, The Netherlands). Twenty-four heart phases and 34 slices were recorded at a spatial resolution of 1.75x1.75x1.75 mm^3.

The image reconstruction problem was solved iteratively using a least-squares solver implemented in Matlab (The Mathworks, Natick, USA) and run on standard PC hardware. Reconstruction times were in the order of 30 minutes per heart phase. Streamline visualization was performed using dedicated software (GyroTools, Zurich, Switzerland).

Results

Figures 1 shows the comparison of noise-corrupted CFD data before and after divergence-free image reconstruction. Clear improvements of the flow pattern in cross-sections and of streamline visualizations were observed. Both the absolute value and the direction of vector field points are corrected for, which is reflected in a decrease of the root-mean-square error (RMSE) from 17.2% to 2.8% relative to the noise-free data. Results from an exemplary in-vivo experiment are shown in Figure 2. An overall improvement of flow patterns in cross-sections and streamline visualization is seen. In particular areas in smaller cross-sections such as the branching arteries are markedly improved yielding an increase in the number and length of streamlines following these vessels (Figure 2c).

Discussion

In this work an approach to divergence-free image reconstruction based on the combination of normalized convolution and tailored radial basis functions has been presented. Comparison of reconstructed CFD and in-vivo data relative to conventional processing has demonstrated significant improvements in vector field representations. It is noteworthy that despite the locality of the approach and hence some remaining discontinuities of the divergence-free constraint across the entire flow domain, significantly enhanced flow fields are reconstructed. The method presented here holds great promise to leverage the clinical usefulness of time-resolved 3D velocity mapping as it potentially permits reconstruction from fewer data points and hence enables reduced scanning times.

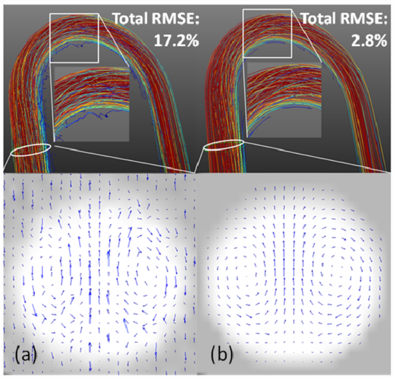

Figure 1: Streamline visualization of U-bend tube and representation of flow patterns in cross-sections of (a) CFD data with added noise and (b) CFD data after divergence-free image reconstruction.

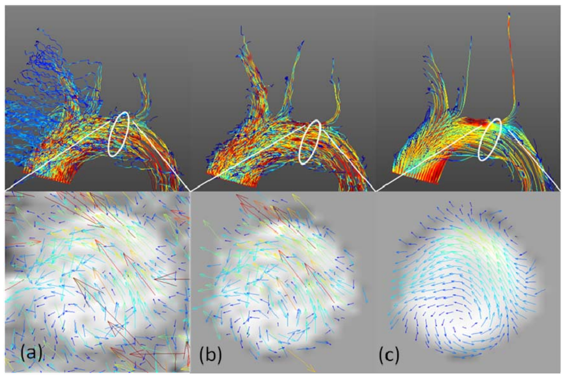

Figure 2: Streamline visualization in the aortic arch and in selected cross-sections for (a) original data, (b) original data after masking to respect boundary condition and (c) data after divergence-free image reconstruction.

References: [1] P.J.Kilner et al., JCMR 2007;9(4):723-8.; [2] O.Friman et al., ISMRM 2010;1334; [3] D.Giese et al., ISMRM 2010;72; [4] S.Lowitzsch, Texas A&M University 2002; [5] O.Škrinjar et al. , IEEE 2009;978-1-4244-3932-4/09/; [6] H.Haraldsson et al., JMRI 2008;28:604-611.